IEEE Access
Multidisciplinary | Rapid Review | Open Access Journal

Received November 6, 2019, accepted December 9, 2019, date of publication December 20, 2019, date of current version January 21, 2020.

Digital Object Identifier 10.1109/ACCESS.2019.2961184

A Fast Epipolar Line Matching Method Based on 3D Spherical Panorama

SHUAI LIU[1], JUN CHEN[2], MIN SUN[3], LINGLI ZHAO[1], AND XIANG WEI[1]
[1]School of Engineering, Honghe University, Mengzi 661100, China
[2]National Geomatics Center of China, Beijing 100048, China
[3]Institute of Geographic Information System and Remote Sensing, Peking University, Beijing 100871, China

Corresponding author: Lingli Zhao (zhaolingli_csu@126.com)

This work was supported in part by the National Natural Science Foundation of China under Grant 41761079, in part by the Universities Joint Special Foundation of Yunnan Provincial Science and Technology Department in China under Grant 2018FH001-046, Grant 2018FH001-056, and Grant 2017FH001-06, in part by the key Projects of the Universities Joint Special Foundation of Yunnan Provincial Science and Technology Department in China ''Study on the estimation method of pomegranate yield based on machine learning geometric feature panoramic image pattern recognition'', in part by the Young and Middle-Aged Academic and Technical Leader Reserve Project of Yunnan Province in China under Grant 201905C160014, and in part by the Top Young Talent Project of Yunnan Province in China.

ABSTRACT A fast epipolar line matching method based on 3D spherical panorama is proposed in this paper in order to overcome the low automation degree of feature matching in applying the 3D panoramic model measurement. First, the search scope of panoramic image matching was restricted from 2D to 1D strip-shaped buffer zone through the epipolar constraints. The search scope was further refined using color invariant correlation coefficient. Finally, a matching calculation model was constructed based on features to complete the panoramic feature matching. The experiment verified the effectiveness and feasibility of the proposed method in reducing the mismatching of spherical panoramic features. The proposed method also effectively solved the automatic search for corresponding points and resolved geometric information. The findings help lay a solid foundation for the resampling and measurement of the panoramic measurement model and the generation of depth maps.

INDEX TERMS CSIFT, color invariant, epipolar line, image matching, spherical projective geometry.

I. INTRODUCTION

Image matching is a core technology that realizes automatic search for corresponding points and the automatic resolution of geometric information in digital photogrammetry and computer vision. Image matching has two phases. First, determining 3D stereo image parameters is completed using Scale-Invariant Feature Transform (SIFT) and its improved algorithm [1], [2], optical flow clustering [3], [4], color invariant [5]–[9], and constrained gross error elimination of Ransac [10]–[12]. Second, re-matching measurement performed using the existing 3D stereo image parameters. The two matching types are consistent in essence, but the second feature matching can improve matching efficiency by constraining the existing 3D image parameters. The present image matching is realized via pinhole camera and satellite images, panoramic image with 360° field of view, and focus on modeling of panoramic image pair model [13]–[18] to resolve stereopair parameters. However, other studies have investigated feature matching in re-sampling measurement, which has become a critical problem in stereo-panoramic application.

The current panoramic image matching work was completed by establishing constraint conditions based on initial matching, including vehicle-mounted system Global Positioning System/Inertial Measurement Unit (GPS/IMU) data [10]–[12], epipolar line, optical flow, scale, sky point and other multi-combinational constraint conditions [4], or kinematic relation satisfying some conditions and features [11], or matching through accurate camera calibration and extraction of connection points [12], [19]–[24]. Once the stereopair is completed, the search problem in matching can be reduced from two to one dimension by establishing the epipolar constraints. Moreover, matching search space is restricted, including between parallel curves [16] or rectangular range, derivation of epipolar equation [14], [16], verification [13], [14], and distribution [16].

The current study focuses on completing the matching work by establishing the epipolar constraints using existing 3D image parameters after the panoramic stereo model is constructed. As the panoramic image is spliced and seamed in 360°, frequency change may occur in different target objects in the image at varying degrees. The existing

The associate editor coordinating the review of this manuscript and approving it for publication was Tallha Akram.

measuring and matching methods, such as gray information measurement method [25], can easily lead to mismatching. Moreover, gross errors [4], [26], [27] caused by texture redundancy and the nonuniform frequency change of panoramic image cannot be solved using feature matching algorithms like SIFT [1], [2], [28] or Speeded Up Robust Features (SURF) [29], [30]. In comparison, the color invariant-based measurement method [5]–[9] can maximize the color information of the image and avoid mismatching when sequential panoramic images collected at the same time are approached.

Given the above situation, a fast epipolar line matching method based on 3D spherical panorama was proposed in the current paper. First, the epipolar constraints could be established according to epipolar trajectory, and the search scope of corresponding points was restricted in the strip-shaped buffer zone through the epipolar constraints. Second, the color invariant correlation coefficient was proposed, then regions was divided along the epipolar line, and the coefficient comparison between the matching point and search region was performed, further reducing the matching scope. Finally, in the five regions with the maximum correlation coefficient, accurate matching was realized after the comprehensive matching method was constructed based on Color Scale-Invariant Feature Transform (CSIFT) features. The experiment verified the effectiveness and feasibility of the proposed method. According to the findings, the method also reduced the mismatching of spherical panoramic features, effectively eliminating mismatching and achieving fast matching. The results help lay a solid foundation for the resampling and measurement of the panoramic measurement model and the generation of depth maps in the future.

II. GEOMETRIC MAPPING RELATIONS OF EPIPOLAR LINES UNDER SPHERICAL PROJECTION

The mapping relation between point P' on the sphere and point p' on the panoramic image is constructed here [16], [22]–[24]. Formula (1) presents the corresponding relation between pixel coordinates $p(x, y)$on the image plane and the angle parameters of the sphere. Formula (2) presents the corresponding relation between the 3D point coordinates $P(X, Y, Z)$of the sphere and spherical angle parameters (ϕ, θ).

$$\begin{cases} x = R \cdot \phi \\ y = R \cdot \theta \\ R = a/2\pi \end{cases} \tag{1}$$

$$\begin{cases} X = R \cdot \sin\phi \cdot \sin\theta \\ Y = R \cdot \cos\phi \cdot \sin\theta \\ Z = R \cdot \cos\theta \end{cases} \tag{2}$$

Through a simple derivation according to Formulas (1) and (2), the corresponding relation between 2D point $p(x, y)$ and 3D point $P(X, Y, Z)$ on the sphere can be obtained as follows:

$$\begin{cases} X = R \cdot \sin\dfrac{x}{R} \cdot \sin\dfrac{y}{R} \\ Y = R \cdot \cos\dfrac{x}{R} \cdot \sin\dfrac{y}{R} \\ Z = R \cdot \cos\dfrac{y}{R} \end{cases} \tag{3}$$

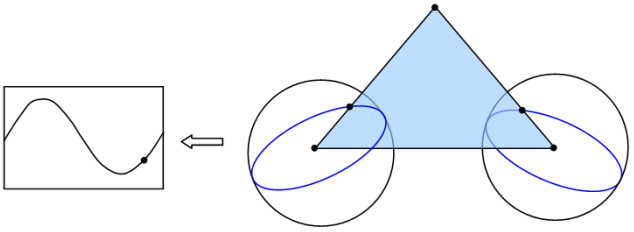

FIGURE 1. Geometric mapping diagram of the spherical epipolar relation.

The epipolar relation between the corresponding points P_1 and P_2 can be established as shown in Figure 1. The panoramic epipolar line is a large arc curve [16]. The coordinates $(X'Y'Z')^T$ of point P_1 under the left panoramic sphere coordinate system can be solved by using Formula (3).

The coordinates of point P under the right panoramic sphere coordinate system are represented by $(X_pY_pZ_p)^T$. The value of the baseline C_1C_2 is set as $B(b_xb_xub_xv)^T$, and the rotation parameters of right panoramic sphere relative to left panoramic sphere are (Φ, Ω, K). The rotation matrix R of the left panoramic sphere coordinates to the right panoramic sphere coordinates is shown in Formula (4).

$$R = inv\left(\begin{pmatrix} \cos\Phi & 0 & -\sin\Phi \\ 0 & 1 & 0 \\ \sin\Phi & 0 & \cos\Phi \end{pmatrix} \cdot \begin{pmatrix} 1 & 0 & 0 \\ 0 & \cos\Omega & -\sin\Omega \\ 0 & \sin\Omega & \cos\Omega \end{pmatrix} \cdot \begin{pmatrix} \cos K & -\sin K & 0 \\ \sin K & \cos K & 0 \\ 0 & 0 & 1 \end{pmatrix}\right) \tag{4}$$

Based on the solved R, the coordinates of point P_1 under the right panoramic sphere coordinate system can be calculated as shown in Formula (5).

$$\begin{pmatrix} X_P \\ Y_P \\ Z_P \end{pmatrix} = R \cdot \begin{pmatrix} X' - b_x \\ Y' - b_x \cdot \mu \\ Z' - b_x \cdot v \end{pmatrix} \tag{5}$$

Under the right panoramic sphere coordinate system, the coordinates of point C_1 are shown in Formula (6) below.

$$\begin{pmatrix} X_{C1} \\ Y_{C1} \\ Z_{C1} \end{pmatrix} = R \cdot \begin{pmatrix} 0 - b_x \\ 0 - b_x \cdot \mu \\ 0 - b_x \cdot v \end{pmatrix} = -b_x \cdot R_2 \cdot \begin{pmatrix} 1 \\ \mu \\ v \end{pmatrix} \tag{6}$$

On the precondition that points P_1, C_1, and P_2 are already known, the trajectory equation of the corresponding epipolar line can be solved according to the deriving [16] shown below.

$$\begin{cases} a_1 = -\dfrac{1}{X_{C1}} \cdot (a_2 \cdot Y_{C1} + Z_{C1}) \\ a_2 = \dfrac{X_{C1} \cdot Z_P - X_P \cdot Z_{C1}}{X_P \cdot Y_{C1} - X_{C1} \cdot Y_P} \\ \phi'' = \arctan\left(-\dfrac{1}{a_1 \cdot \sin\theta'' + a_2 \cdot \cos\theta''}\right) \end{cases} \tag{7}$$

The central points $C_1(Xc_1, Yc_1, Zc_1)^T$ and $P(X_p, Y_p, Z_p)^T$ on the left sphere are substituted into the above formula to determine coefficients a_1 and a_2. The relation between θ'' and φ'' is presented in Formula (7), where θ'' is the parameter with

value range of 0–2π, and the value of φ' can be determined through θ'', that is, the trajectory formed by the corresponding epipolar line in the left virtual sphere.

III. COMPREHENSIVE MATCHING ALGORITHM BASED ON THE GEOMETRIC CONSTRAINTS OF EPIPOLAR LINE

Two panoramic images were shot according to a previously discussed method [16]. Over eight groups of corresponding points were matched to complete the construction of the panoramic stereopairs and obtain translation and rotation parameters (u, v, Φ, Ω, K). When a point in the panoramic image is already known, the trajectory of the epipolar line where the corresponding point is located can be calculated according to Section 2. The epipolar trajectory calculation of the corresponding point refers to the unfolding from the sphere to image plane with possible deformation. The epipolar constraints can be established according to the already obtained epipolar trajectory, and the search of corresponding points is controlled within the region near the epipolar line. This step reduces the matching scope.

Matching difficulty and the complexity of panoramic images are aggravated due to specific frequency change nonuniformity characteristics, such as geometric projection, rotation transformation, scaling relation, and texture redundancy. Such algorithms as SIFT and SURF can achieve good effects when they are used to extract gray features and to maintain the rotation transformation. However, under similar texture or nonuniform scale changes, they show certain limitations. The CSIFT algorithm [5], [6] can maintain the characteristics of SIFT and fully take advantage of color information as well as the geometric features, and process. CSIFT can also improve texture redundancy to solve the frequency change nonuniformity problem of panoramic images. Hence, in the current study, a matching method improved from the CSIFT algorithm was designed based on the color invariant correlation coefficient constrained by the spherical panoramic epipolar line. Color and shape features were considered in this improved method. The spherical panoramic epipolar constraints, image color, and shape features were also fully considered, as shown in Figure 2. First, the epipolar line parameters of a panoramic image were solved accordingly [16]. Points were taken from the reference image according to epipolar line parameters, and the search scope of the large arc constituted by corresponding points was determined using Formula (7) shown in Section 2. Subsequently, the search scope was refined based on the color invariant correlation coefficient, and accurate matching was realized after the comprehensive matching method was constructed based on CSIFT.

A. COLOR INVARIANTS

According to Kubelka-Munk theory [5], the light environment and geometric parameters of the object are unchanged in the imaging process, this is called color invariant H [5] and

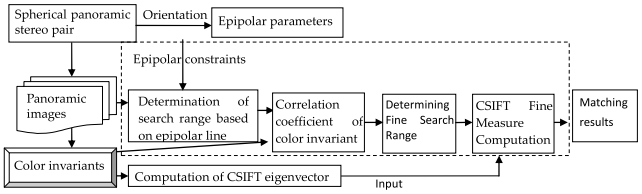

FIGURE 2. Schematic diagram of the idea of the proposed matching method.

the formula is given by

$$H = \frac{E_\lambda}{E_{\lambda\lambda}} = \frac{\partial E/\partial\lambda}{\partial^2 E/\partial\lambda^2} = \frac{\partial R_\infty(\lambda, x)/\partial\lambda}{\partial^2 R_\infty(\lambda, x)/\partial\lambda^2} = f[R_\infty(\lambda, x)] \tag{8}$$

where $E(\lambda, x)$ is reflective spectrum at the observational point; E_λ and $E_{\lambda\lambda}$ are the first- and second-order derivatives of λ, respectively; and the corresponding relations of E, E_λ, and $E_{\lambda\lambda}$ with the RGB component of the image is approximated as shown below.

$$\begin{bmatrix} E \\ E_\lambda \\ E_{\lambda\lambda} \end{bmatrix} = \begin{bmatrix} 0.06 & 0.63 & 0.27 \\ 0.30 & 0.04 & -0.35 \\ 0.34 & -0.60 & 0.17 \end{bmatrix} \times \begin{bmatrix} R \\ G \\ B \end{bmatrix} \tag{9}$$

Color invariant H of the colored image can be solved through Formulas (8) and (9).

Color invariant is not related to observation place, surface orientation, light intensity, and reflection coefficient. Moreover, its matching effect is good when applied to distinguish features with approximate textures but different colors.

B. DETERMINATION OF THE SEARCH SCOPE OF CORRESPONDING POINTS THROUGH THE EPIPOLAR CONSTRAINTS

Theoretically, featured corresponding points should be on an epipolar line. Due to the possible deformation from the the spherical projection to the image plane, mismatching may still exist after rough matching. Hence, the epipolar trajectory is expected to deviate from the corresponding feature points. Therefore, the search region with height being 3% to 5% of the image width (60 pixels used in this paper) is initiated at the epipolar trajectory, as shown in Figure 3. According to the green feature points in the blue region selected in the left sphere, the corresponding epipolar line (black line in the red annular region) in the right sphere can be determined, and the red annular region is opened as the matching search zone. The matching search zone is unfolded from the sphere to the image plane, as shown by the curve zone at the lower right of Figure 3. This matching zone should present the zigzag shape at the lower left of Figure 3.

C. MATCHING COMPARISON BASED ON THE COLOR INVARIANT CORRELATION COEFFICIENT

The matching search scope can be restricted within the epipolar zone (Figure 3) through the epipolar constraints. The length of the epipolar zone is generally 1.0 to 1.5 times of the image length, and the scope is still broad. Therefore,

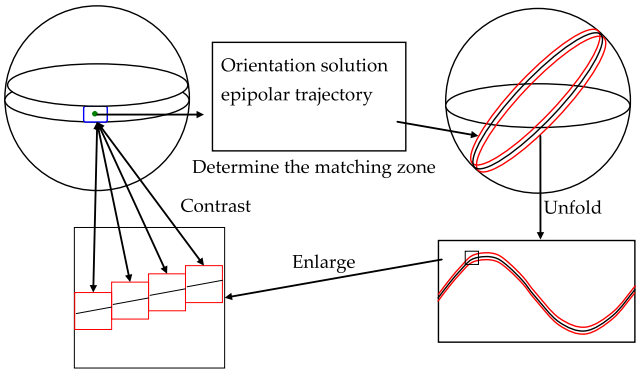

FIGURE 3. Determination of the matching search zone based on the epipolar line and comparative graph.

a matching algorithm based on color invariant correlation coefficient was proposed in this paper. The coefficient comparison between the matching point and search region was performed (double-sided arrows in Figure 3, comparison between the blue and red line regions), further reducing the matching scope.

According to statistical theory, the correlation coefficient-based image matching algorithm is a stable gray-scale matching algorithm that is used to judge the similarity of certain window pixels in two images. If the regional color invariants are taken as input information in the two regions and then substituted into correlation coefficient solving formula, the correlation coefficient of the color invariant information can be obtained. This information is called the color invariant correlation coefficient ρ_H, and its formula is shown in Formula (10). Such a coefficient can be used to compare the correlation in color information between two regions. The color information in the peripheral regions of the corresponding points in the two images should have the highest correlation. As demonstrated in the experiment on different region sizes, when the region size exceeds 150 pixels or is lower than 30 pixels, the color invariant correlation coefficient does not have enough degree of distinction. The results showed that the 100-pixel region is the most stable, thus justifying the choice of 100-pixel size region for comparing the regional widths.

$$\begin{cases} \rho_H = \dfrac{\sigma_{H_1H_2}}{\sqrt{\sigma_{H_1}\sigma_{H_2}}} \\ \sigma_{H_1} = \dfrac{1}{n\cdot m}\sum_{i=1}^{n}\sum_{j=1}^{m} H_1(x,y)^2 - \bar{H}_1^2 \\ \sigma_{H_2} = \dfrac{1}{n\cdot m}\sum_{i=1}^{n}\sum_{j=1}^{m} H_2(x,y)^2 - \bar{H}_2^2 \\ \sigma_{H_1H_2} = \dfrac{1}{n\cdot m}\sum_{i=1}^{n}\sum_{j=1}^{m} H_1(x,y)H_2(x,y) - \bar{H}_1\bar{H}_2 \\ \bar{H}_1 = \dfrac{1}{n\cdot m}\sum_{i=1}^{n}\sum_{j=1}^{m} H_1(x,y) \\ \bar{H}_2 = \dfrac{1}{n\cdot m}\sum_{i=1}^{n}\sum_{j=1}^{m} H_2(x,y) \end{cases} \tag{10}$$

The color invariants $H_1(x, y)$ and $H_2(x, y)$ of the reference image $I_1(x, y)$ and to-be-rectified image $I_2(x, y)$ are respectively solved using Formula (8). Here, H_1 and H_2 are taken as the feature information of I_1 and I_2, respectively, to replace the gray information for input. The specific steps are described below.

1) REGIONAL MATCHING BASED ON THE COLOR INVARIANT CORRELATION COEFFICIENT

Within the trajectory search region (matching search zone in Figure 3), the red annulus is segmented into n regions with the approximate length and width along the direction of the epipolar line ($n = 40$). The regional size is 100 px * 100 px as, as shown in Figure 3, and is presented as a zigzag shape.

For the matching (blue region in Figure 3) and to-be-matched regions (n segmented regions in Figure 3), color invariants H_1 and H_2 are taken as input information. Subsequently, ρ_H is solved according to Formula (10), followed by a comparison. The five regions with the maximum correlation coefficient are then reserved for the next refined matching.

2) CONSTRUCTION OF SCALE SPACE

The color invariant is taken as image information similar to the SIFT algorithm. Laplacian of Gaussian (LOG) is used to calculate convolution within the image scape, from which the Gaussian (LOG) pyramid is established. The extreme point is detected as well.

3) DETERMINATION OF THE FEATURE POINT

The local extreme value point in the Hessian matrix (formula 11) after scale normalization is sought. The comparison among the candidate and 26 adjacent points results in the accurate identification of the feature point's position.

$$H\_h = \begin{bmatrix} D_{xx} & D_{xy} \\ D_{xy} & D_{yy} \end{bmatrix} \tag{11}$$

4) DETERMINATION OF THE PRINCIPAL DIRECTION OF FEATURE POINTS

The local image feature (gradient) of the critical point is used to indicate a principal direction (the direction with the maximum gradient) for each critical point. The $g(x, y)$ is the gradient value of feature point and $\theta(x, y)$ is gradient direction of feature point. The scale used by L is the scale space wherein each feature point is located and its information source is color invariant H.

$$\begin{cases} g(x,y) \\ = \sqrt{(L(x+1,y)-L(x-1,y))^2+(L(x,y+1)-L(x,y-1))^2} \\ \theta(x,y) = \arctan 2\left(\dfrac{L(x,y+1)-L(x,y-1)}{L(x+1,y)-L(x-1,y)}\right) \end{cases} \tag{12}$$

5) GENERATION OF THE EIGENVECTOR

On the image expressed by color invariant, centering on the feature point leads to the selection of the peripheral

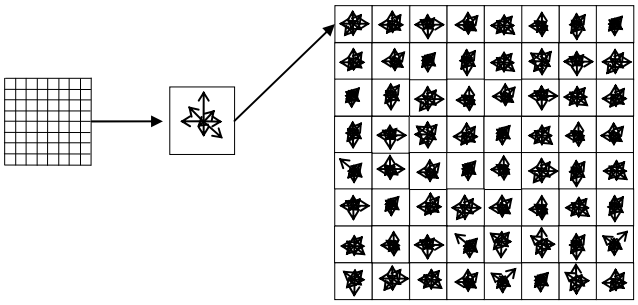

FIGURE 4. Generation of the CSIFT feature descriptor.

(a) Indoor (b) Outdoor

FIGURE 5. Two sets of spherical panoramic images.

(a) Indoor (b) Outdoor

FIGURE 6. Schematic diagram of the corresponding epipolar trajectory of the feature point, namely, the matching regional division.

64 × 64 region, which is divided into 8 × 8 subregions, as shown in Figure 4. In each subregion, the 8-directional (0°, 45°, 90°, 135°, 180°, 225°, 275°, and 315°) gradients are calculated through Formula (13). A weight value is added based on the original algorithm. The color invariant information is multiplied by the weight value along the gradient direction and then accumulated to obtain an 8D eigenvector (Figure 4). This weight value is reduced outward with the feature point being the center. Hence, the contribution of pixel gradients close to the central point to the final eigenvector is increased, whereas the contribution of pixel gradients away from the central point to the eigenvector is reduced.

$$\begin{cases} g(x,y) \\ = \sqrt{(L(x+1,y)-L(x-1,y))^2+(L(x,y+1)-L(x,y-1))^2} \\ \theta(x,y) = \arctan 2(\dfrac{L(x,y+1)-L(x,y-1)}{L(x+1,y)-L(x-1,y)}) \end{cases} \tag{13}$$

The 8D eigenvectors of the right 8 × 8 = 64 subregions in Figure 4 are successively combined according to their positions to obtain a 64 × 8 = 512-dimensional vector, which is the CSIFT feature description vector. In addition, the length of the SIFT eigenvector is used to perform normalization processing of the length of each element such that the eigenvector has strong robustness.

6) FEATURE MATCHING

The SIFT eigenvector S of the matching point and SIFT eigenvector $T_k(k = 1, 2, 3, \ldots N)$ of the search point are normalized. The Euclidean distance between S and eigenvector $T_k(k = 1, 2, 3, \ldots N)$ of the to-be-matched feature point is calculated according to Formula (14) as $(d_1, d_2, d_3, \ldots d_N)$. If the ratio of minimal value d_i to secondary minimal value d_j in $(d_1, d_2, d_3, \ldots d_N)$ is smaller than one threshold value (taken as 0.8 in this paper), then the feature point S matches with feature point T_i.

$$d = \sqrt{\sum_{j=1}^{128} (S_{x,y}(j) - T_{x,y}(j))^2} \tag{14}$$

IV. EXPERIMENT AND DISCUSSION

The shooting experiments were separately conducted inside and outside a building with a camera model, Canon EOS 5D Mark, and fisheye lens, Cannon EF8-15mm; the camera head was JTS-Rotator SPH. An ordinary tripod and central leveling were also used. Six photos were shot at each position every 60°, and the photos were then spliced into two spherical panoramic images using commercial software. These photos were taken as an example to verify the algorithm proposed in this paper. Station spacing was about 7 m and was respectively arranged at two sides of the orientation control device (red circle in Figure 5).

To comprehensively verify the matching accuracy, precision, and efficiency of the proposed method, the experiment was performed indoor and outdoor in two groups. The construction of the panoramic stereopairs was descripted in [16]. Over eight groups of corresponding points were acquired to complete the construction of the panoramic stereopairs and obtain translation and rotation parameters (u, v, Φ, Ω, K).

Firstly, the epipolar parameters were solved for each group of panoramic images. The feature points (red reticule in Figure 6) were selected in the reference image. The epipolar trajectory was calculated according to the epipolar parameters as represented by the black dotted line near the red region in Figure 6. The search scope could be determined based on the epipolar line. In Figure 6, 30 equally sized regions could be divided along the epipolar trajectory for matching (n = 30).

The color invariant correlation coefficients between the region centering on the feature point in the reference image

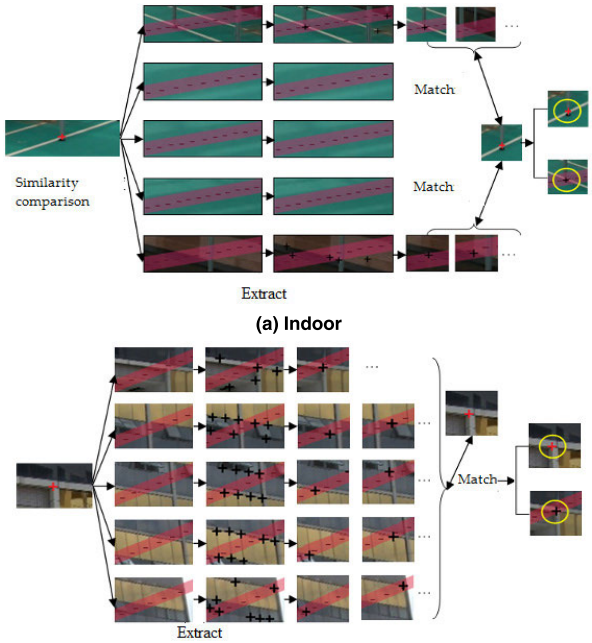

FIGURE 7. Fine matching schema.

TABLE 1. Comparison results of the matching methods.

	Methods	Pairs	Correct pairs	Time/ Seconds	Accuracy
Indoor	Gray match	117	73	4.3	62.4%
	SIFT	142	115	7.9	81.0%
	SURF	145	121	6.7	83.4%
	CSIFT	147	124	7.6	84.4%
	Improved CSIFT	152	137	5.8	90.1%
Outdoor	Gray match	109	63	4.1	57.8%
	SIFT	121	96	7.3	79.3%
	SURF	119	95	6.6	79.8%
	CSIFT	125	102	7.2	81.6%
	Improved CSIFT	139	126	5.4	90.6%

and 40 regions were calculated. Five regions with the maximum correlation coefficients were selected (5 regions in the middle of Figure 7). Then, the feature points within the scope of epipolar trajectory in the five regions were extracted and matched with the reference image, until the matching result was obtained. Taking the outdoor experiment as an example, the experimental matching result is shown in Figure 8.

The proposed method was compared with the gray matching method, SIFT, SURF, and CSIFT, and the experimental results are shown in Table 1.

The experimental comparison results showed that the matching accuracy of gray correlation coefficient was the lowest with the shortest matching time. The SIFT matching method spent the longest time with moderate matching accuracy, and the improved CSIFT method had the highest matching accuracy. The adoption of the color invariant correlation coefficients to screen matching regions resulted in the shortest consumed time.

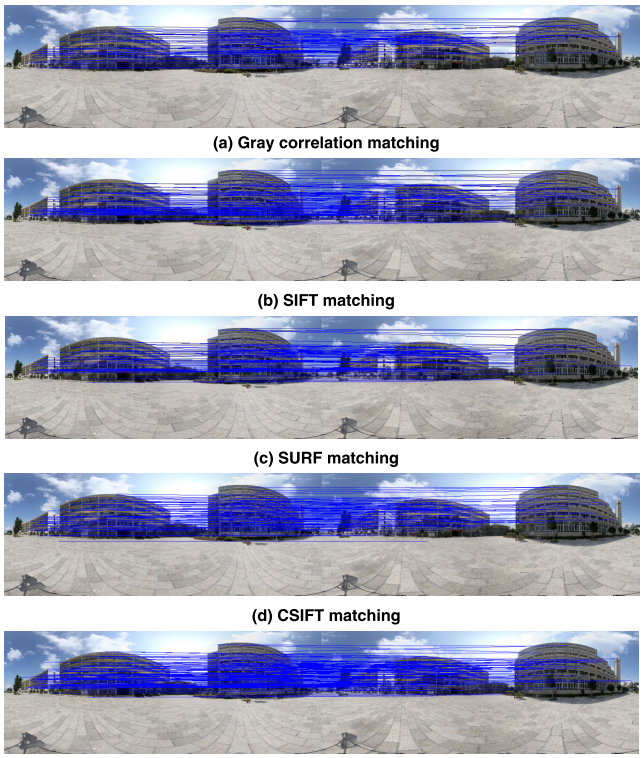

FIGURE 8. Comparison results of outdoor matching method.

V. CONCLUSION

In this work, epipolar constraints were utilized to overcome the the feature matching problems arising from the 3D spherical panoramic image measurement.This way, the search scope of the corresponding points was reduced, and the CSIFT method was also improved based on the color invariant correlation coefficients. The image structure and color information were then fully utilized to reduce mismatching caused by texture redundancy and scale nonuniformity of panoramic images. Thus, the matching reliability and efficiency were significantly improved. The experiment proved the feasibility and effectiveness of the proposed comprehensive matching method with the epipolar geometric constraints. The proposed method also eliminated the mismatching of spherical panoramic features and effectively solved automatic searching for corresponding image points and quickly resolving geometric information in the image matching process. The results help lay a solid foundation for the sampling and measurement of the panoramic model and generation of depth maps in the future. In terms of limitation, the proposed method was influenced by the relative positioning result, which could lead to the mismatching of points near the baseline when applied to matching of corresponding points.

REFERENCES

[1] M. Gong, S. Zhao, L. Jiao, D. Tian, and S. Wang, "A novel coarse-to-fine scheme for automatic image registration based on SIFT and mutual information," *IEEE Trans. Geosci. Remote Sens.*, vol. 52, no. 7, pp. 4328–4338, Jul. 2014.

[2] F. Dellinger, J. Delon, Y. Gousseau, J. Michel, and F. Tupin, "SAR-SIFT: A SIFT-like algorithm for SAR images," *IEEE Trans. Geosci. Remote Sens.*, vol. 53, no. 1, pp. 453–466, Jan. 2015.
[3] I. Labutov, C. Jaramillo, and J. Xiao, "Generating near-spherical range panoramas by fusing optical flow and stereo from a single-camera folded catadioptric rig," *Mach. Vis. Appl.*, vol. 24, no. 1, pp. 133–144, 2013.
[4] Z. Zhengpeng, J. Wanshou, and Z. Jing, "An image match method based on optical flow feature clustering for vehicle-borne panoramic image sequence," *Acta Geodaetica et Cartographica Sinica*, vol. 43, no. 12, pp. 1266–1273, 2014.
[5] A. E. Abdel-Hakim, and A. A. Farag, "CSIFT: A SIFT descriptor with color invariant characteristics," in *Proc. IEEE Comput. Soc. Conf. Comput. Vis. Pattern Recognit. (CVPR)*, vol. 2, Jun. 2006, pp. 1978–1983.
[6] I. Kviatkovsky, A. Adam, and E. Rivlin, "Color invariants for person reidentification," *IEEE Trans. Pattern Anal. Mach. Intell.*, vol. 35, no. 7, pp. 1622–1634, Jul. 2013.
[7] R. R. Varior, G. Wang, J. Lu, and T. Liu, "Learning invariant color features for person reidentification," *IEEE Trans. Image Process.*, vol. 25, no. 7, pp. 3395–3410, Jul. 2016.
[8] J. Chen, Q. Li, Q. Peng, "CSIFT based locality-constrained linear coding for image classification," *Pattern Anal. Appl.*, vol. 18, no. 2, pp. 441–450, 2015.
[9] L. Huanaing, X. Yi, and F. Sizhou, "UAV image registration algorithm using color invariant and AKAZE feature," *Acta Geodaetica et Cartographica Sinica*, vol. 46, no. 7, pp. 900–909, 2017.
[10] T. Cui, S. Ji, and J. Shan, "Line-based registration of panoramic images and LiDAR point clouds for mobile mapping," *Sensors*, vol. 17, no. 1, p. 70, 2017.
[11] J. Shunping and S. Yun, "Image matching and bundle adjustment using vehicde-based panoramic camera," *Acta Geodaetica et Cartographica Sinica*, vol. 42, no. 1, pp. 94–100, 2013.
[12] Y. Shi, S. Ji, and Z. Shi, "GPS-supported visual SLAM with a rigorous sensor model for a panoramic camera in outdoor environments," *Sensors*, vol. 13, no. 1, pp. 119–136, 2013.
[13] L. Shuai, C. Jun, S. Min, and Z. Lingli, "Measurable panorama construction based on binocular spherical projective geometry," *J. Comput.-Aided Des. Comput. Graph.*, vol. 27, no. 4, pp. 657–665, 2015.
[14] X. Donghai, Z. Ruofei, and W. Yu, "Relative pose estimation and accuracy verification of spherical panoramic image," *Acta Geodaetica et Cartographica Sinica*, vol. 46, no. 11, pp. 1822–1829, 2017.
[15] W. Zhixuan, Z. Ruofei, and X. Donghai, "Automatically measuring the coordinates of streetlights in vehicle-borne spherical images," *J. Image Graph.*, vol. 23, no. 09, pp. 1371–1381, 2018.
[16] L. Shuai, C. Jun, S. Min, and Z. Lingli, "The derivation and analysis of spherical panorama Epipolar line based on essential matrix," *J. Comput.-Aided Des. Comput. Graph.*, vol. 28, no. 5, pp. 785–794, 2016.
[17] C. Reinbacher, G. Munda, and T. Pock, "Real-time panoramic tracking for event cameras," in *Proc. IEEE Conf. Comput. Photography (ICCP)*, May 2017, pp. 1–9.
[18] M. Rosenthal, W. Wu, and E. Klassen, "Spherical regression models using projective linear transformations," *J. Amer. Stat. Assoc.*, vol. 109, no. 508, pp. 1615–1624, 2014.
[19] T. Luhmann and W. Tecklenburg, "Bundle orientation and 3-D object reconstruction from multiple-station panoramic imagery," *Int. Arch. Photogram., Remote Sens. Spatial Inf. Sci.*, vol. 34, no. 5, pp. 181–186, 2002.
[20] T. Luhmann and W. Tecklenburg, "3-D object reconstruction from multiple-station panorama imagery," *Int. Arch. Photogram., Remote Sens. Spatial Inf. Sci.*, vol. 34, no. 5/W16, pp. 1–8, 2004.
[21] T. Luhmann, "Panorama photogrammetry for architectural applications," *Mapping*, no. 139, pp. 40–45, 2010.
[22] G. Fangi, "The multi-image spherical panoramas as a tool for architectural survey," in *Proc. 21st CIPA Symp.* Athens, Greece: ISPPS International Archive, 2011, vol. 36, no. 5/C53, pp. 21–26.
[23] G. Fangi, "Further developments of the spherical photogrammetry for cultural heritage," in *Proc. 22nd CIPA Symp.* Kyoto, China: ISPPS International Archive, 2009, pp. 11–15.
[24] G. Fangi, "Multiscale multiresolution spherical photogrammetry with long focal lenses for architectural surveys," *Int. Archives Photogram., Remote Sens. Spatial Inf. Sci.*, vol. 38, no. 5, pp. 1–6, 2010.
[25] L. Shamir, "A proposed stereo matching algorithm for noisy sets of color images," *Comput. Geosci.*, vol. 33, no. 8, pp. 1052–1063, 2007.
[26] T. Sato, T. Pajdla, and N. Yokoya, "Epipolar geometry estimation for wide-baseline omnidirectional street view images," in *Proc. IEEE Conf. Comput. Vis. Workshops (ICCV Workshops)*, Nov. 2011, pp. 56–63.
[27] Z. Zhengpeng, J. Wanshou, and Z. Jing, "A matching method for vehicle borne panoramic image sequence based on adaptive structure from motion feature," *Acta Geodaetica et Cartographica Sinica*, vol. 44, no. 10, pp. 1132–1141, 2015.
[28] D. G. Lowe, "Distinctive image features from scale invariant feature transform," *Int. J. Comput. Vis.*, vol. 60, no. 2, pp. 91–110, 2004.
[29] H. Bay, T. Tuytelaars, and L. Van Gool, "Surf: Speeded up robust features," in *Proc. Eur. Conf. Comput. Vis.* Berlin, Germany: Springer, 2006, pp. 404–417.
[30] Y. Pang, W. Li, and Y. Yuan, "Fully affine invariant SURF for image matching," *Neurocomputing*, vol. 85, pp. 6–10, 2012.

SHUAI LIU received the B.S., M.S., and Ph.D. degrees in geographic information system from Central South University, Changsha, China, in 2003, 2006, and 2011, respectively. From March 2007 to May 2011, he was a Research Associate with the National Geomatics Center of China. He is currently working with the School of Engineering, Honghe University, Mengzi, China. His research interests include computer vision, 3D modeling, and virtual augmented reality.

JUN CHEN received the B.S. and M.S. degrees in photogrammetry and remote sensing from Wuhan University, in 1983 and 1986, respectively. He has been working with the National Geomatics Center of China, Beijing, since 1995. He is the author of one book and more than 100 articles. His research interests include theory and application of GIS modeling.

MIN SUN received the B.S., M.S., and Ph.D. degrees in survey and mapping engineering from Central South University, China, in 1992, 1995, and 2000. From 2000 to 2002, he was a postdoctoral position at the Institute of Remote Sensing & GIS, Peking University. From July of 2002 to 2004, he worked as a Lecturer with the Institute of Remote Sensing & GIS. From 2004 and 2005, he worked as a Visiting Scholar with the Institute of Computer Science and Applied Mathmatics, CAU of Kiel, Germany. Since July 2006, he has been an Assistant Professor with the Institute of Remote Sensing & GIS. He is the author of one book and more than 50 articles. His research interests include augment reality GIS and UAV remote sensing related image process.

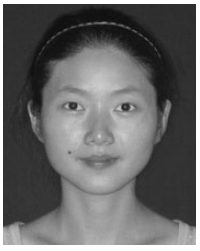

LINGLI ZHAO received the B.S. degree in computer science, and the M.S. and Ph.D. degrees in geographic information system from Central South University, Changsha, China, in 2001, 2006, and 2010, respectively. She is currently working with the School of Engineering, Honghe University, Mengzi, China. Her research interests include 3D modeling, computer vision, and Image processing.

XIANG WEI received the M.S. degree in computational mathematics from Yunnan University, Kunming, China, in 2006. He is currently pursuing the Ph.D. degree with the School of Mathematics and Statistics, Wuhan University. He is currently an Associate Professor with the School of Engineering, Honghe University, Mengzi, China. His research interests include complex networks, nonlinear dynamics, propagation dynamics, and chaos control.